EVOLUTION OF BIOMINERALIZATION

Cooperation between passive and active silicon transporters clarifies the ecophysiology and evolution of biosilicification in sponges

M. Maldonado[1]*, M. López-Acosta[1], L. Beazley[2], E. Kenchington[2], V. Koutsouveli[3], A. Riesgo[3]

The biological utilization of dissolved silicon (DSi) influences ocean ecology and biogeochemistry. In the deep sea, hexactinellid sponges are major DSi consumers that remain poorly understood. Their DSi consumption departs from the Michaelis-Menten kinetics of shallow-water demosponges and appears particularly maladapted to incorporating DSi from the modest concentrations typical of the modern ocean. Why did sponges not adapt to the shrinking DSi availability that followed diatom expansion some 100 to 65 million years ago? We propose that sponges incorporate DSi combining passive (aquaglyceroporins) and active (ArsB) transporters, while only active transporters (SITs) operate in diatoms and choanoflagellates. Evolution of greater silicon transport efficiency appears constrained by the additional role of aquaglyceroporins in transporting essential metalloids other than silicon. We discuss the possibility that lower energy costs may have driven replacement of ancestral SITs by less efficient aquaglyceroporins, and discuss the functional implications of conservation of aquaglyceroporin-mediated DSi utilization in vertebrates.

INTRODUCTION

Silicon (Si), in the form of dissolved silicic acid—often referred to as silicate and hereafter abbreviated as DSi—is an inorganic nutrient instrumental to ocean functioning. Its availability modulates processes as relevant as ocean primary productivity (*1*) and the exchange of CO_2 with the atmosphere (*2*). Regional patterns of DSi availability largely result from the consumption of this nutrient by marine organisms (silicifiers) to build their skeletons of biogenic silica (BSi), with diatom utilization among the best known and quantified (*1*, *3*). However, sponges, radiolarians, silicoflagellates, choanoflagellates, testate amoebae, and chrysophyceans, among others, also consume DSi in the ocean (*4*), but their activity remains poorly quantified and little understood from a physiological and molecular perspective. In the diatoms, the kinetics of DSi uptake have been investigated in a large variety of species, all of which were reported initially to follow a saturable Michaelis-Menten model. It is also that those saturable kinetics shift into nonsaturable uptake when DSi availability drastically increases and/or under particular physiological conditions (*5*, *6*). Likewise, membrane silicon transporters (SITs) incorporating actively ambient DSi into the diatom cell have long been described and, although passive transporters have not been identified yet, a diffusion-based uptake has been described for at least some diatoms at high DSi availability [reviewed in (*7*)]. In contrast, little is known about these physiological and molecular processes in other groups of marine silicifiers. Because diatoms are restricted to the photic zone of the ocean, a major gap in knowledge relative to DSi utilization in the dark ocean by nonphototrophic silicifiers persists. The discoveries that extensive aggregations of highly silicified sponges are common in the deep sea (*8*), that they can accumulate substantial amounts of BSi at the regional scale (*9*, *10*), and that they trigger significant losses of BSi from the ocean (*11*) have raised considerable interest in deciphering how Si is processed in these singular, sponge-dominated, deep-sea systems. The lack of knowledge regarding these processes in sponges currently hinders the ability to understand the Si utilization in the dark ocean and makes it difficult to model adequately the role of the biological component in the marine biogeochemical cycle of silicon (*3*, *11*).

Information on the physiology of DSi consumption by sponges is sparse and derived exclusively from shallow-water species in the class Demospongiae. These studies indicate Michaelis-Menten kinetics but with optimal DSi consumption attained at environmental DSi concentrations of >100 μM (*12*–*16*). Because DSi concentrations higher than 100 μM are virtually never reached in the shallow waters of the modern ocean (*17*), the skeletal growth of all shallow-water demosponges investigated to date is therefore chronically limited by Si availability (*15*, *16*, *18*–*20*). Whether this kinetic limitation also applies to sponges in the class Hexactinellida—deep-sea specialists characterized by impressive siliceous skeletons—remains unknown. The physiology of DSi consumption and the molecular pathways of DSi uptake remain largely uninvestigated in hexactinellids, hampered by impediments to conducting in situ and laboratory experimentation with such relatively large and delicate deep-sea animals. Nevertheless, the interest is enormous. Major differences in the kinetics of DSi utilization between the two major lineages of siliceous sponges (i.e., Demospongiae and Hexactinellida) cannot be discarded, as silicification in demosponges revolves around the activity of the nonsoluble silicatein enzyme (*21*), while the process in hexactinellids appears to be governed by a phylogenetically unrelated, soluble enzyme, glassin (*22*). In addition, because hexactinellids have essentially syncytial organization while demosponges have a conventional cellular organization, the membrane transporters involved in Si utilization may not be shared but may be lineage specific instead. Very little is known on molecular Si transport in demosponges (*23*, *24*) and nothing in hexactinellids. This lack of knowledge obscures the understanding of the evolution of the biosilicification process in the animal kingdom and its relationships to that in other organisms.

[1]Department of Marine Ecology, Center for Advanced Studies of Blanes (CEAB-CSIC), Acceso Cala St. Francesc 14, Blanes 17300, Girona, Spain. [2]Department of Fisheries and Oceans, Bedford Institute of Oceanography, 1 Challenger Dr., Dartmouth, NS, Canada. [3]Department of Life Sciences, The Natural History Museum of London, Cromwell Road, SW7 5BD London, UK.
*Corresponding author. Email: maldonado@ceab.csic.es

Here, we characterized experimentally the kinetics of DSi consumption in the hexactinellid sponge *Vazella pourtalesii* (Schmidt, 1870), a rosellid distributed from ~100 to 935 m in the northwest Atlantic that forms extensive monospecific aggregations on the deep continental shelf off Nova Scotia (Fig. 1A and fig. S1), eastern Canada (*25*). We tested the laboratory-based kinetic model by comparing its predictions to both in situ determinations of DSi consumption rates using incubation chambers (Fig. 1, B to D, and movies S1 and S2) and rates of BSi production derived from individuals of a known age grown in the wild on an artificial substrate (Fig. 1, E and F). In combination with those physiological experiments, we conducted a quantitative large-scale assessment of gene expression as a function of DSi availability. The results of this study offer a mechanistic explanation for the kinetics of DSi utilization in hexactinellids and provide fresh insights into the molecular systems of Si transport and their evolution within sponges and across other silicifying organisms.

RESULTS

Modeling and testing the physiology of DSi consumption

Live sponges were collected using the remotely operated vehicle (ROV) Remotely Operated Platform for Ocean Sciences (ROPOS) and taken to the laboratory for incubation in progressively increasing DSi concentrations (12, 30, 60, 100, 150, 200, and 250 μM DSi; see Materials and Methods). Initially, all 11 assayed individuals increased their DSi consumption rate in response to the progressive increase of DSi availability in the seawater (Fig. 2, A and B, and tables S1 and S2). As also known for demosponges, the DSi consumption rate notably varied among individuals, with an average maximum consumption of 0.106 ± 0.050 μmol Si per

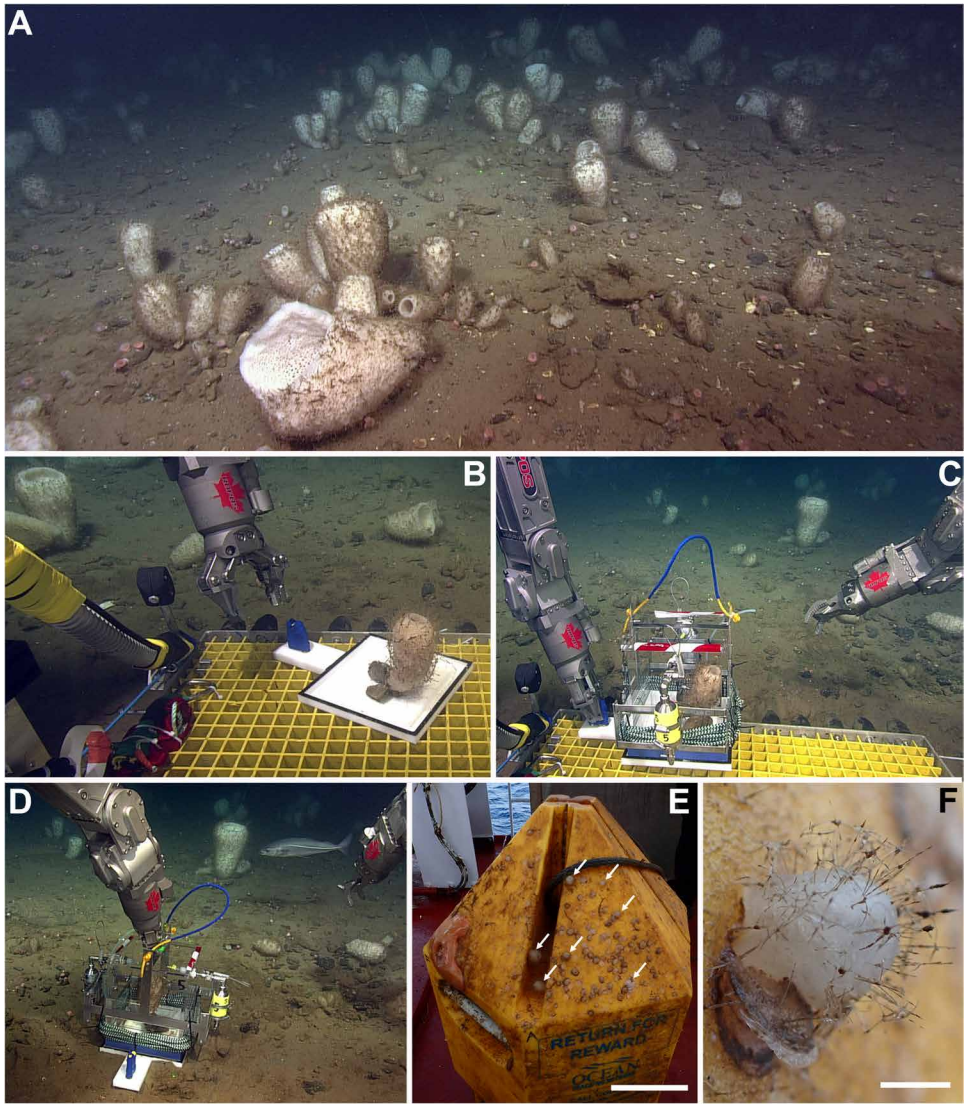

Fig. 1. Imagery depicting various aspects of field work. (**A**) General view of the aggregation of *V. pourtalesii* in the Sambro Bank Sponge Conservation Area in Emerald Basin. (**B**) Collected sponge transferred to the floor piece of the incubation chamber. (**C**) Sponge enclosed in incubation unit, which is being clutched by the ROV arm for deployment on the seabed. (**D**) Incubation unit deployed on the sponge ground. (**E**) Recovered Ocean Tracking Network (OTN) mooring with *V. pourtalesii* (arrows) recruitment. Scale bar, 25 cm. (**F**) Close-up of a sponge recruited on the mooring showing its protruding BSi skeleton. Scale bar, 1 cm. Pictures (A) to (D) are frames from movies extracted and processed by M. Maldonado (CEAB-CSIC). Pictures (E) and (F) were taken by M. Maldonado (CEAB-CSIC).

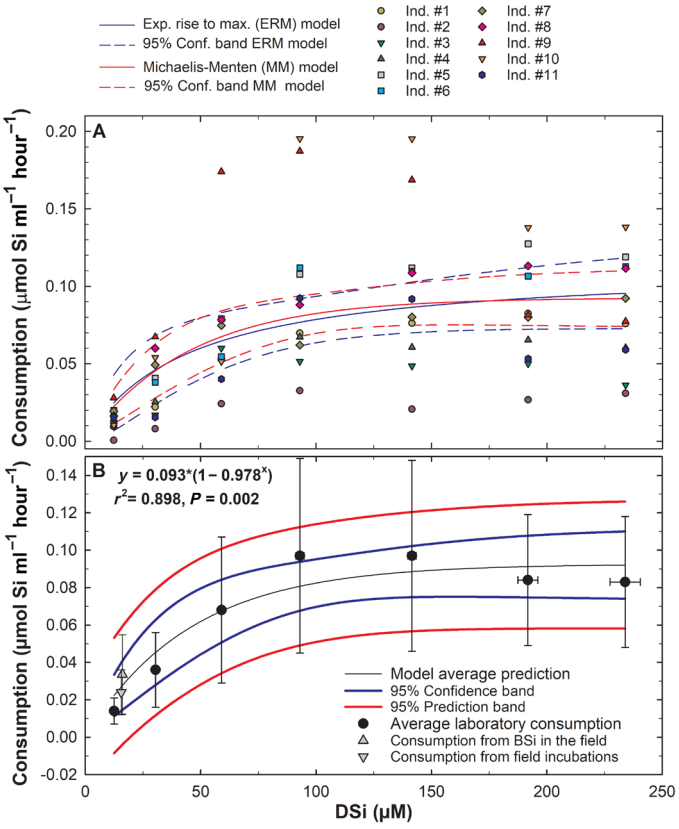

Fig. 2. Summary of DSi consumption as a function of experimental DSi availability. (**A**) DSi consumptions of 11 individuals of *V. pourtalesii* as a function of experimental silicic acid (DSi) concentration in the laboratory. The averaged response fits an ERM model (blue lines) better than a Michaelis-Menten (MM) kinetics (red lines). (**B**) Statistics of the average consumption (±SD) best fitting to an ERM model. Note that DSi consumption calculated both from in situ incubations and from BSi produced under field conditions fall within the 95% confidence band of the model.

milliliter of sponge tissue and per hour (hereafter given as µmol Si ml^{-1} $hour^{-1}$) at an average DSi concentration of 150.9 ± 69.3 µM. Over that concentration threshold, the consumption rate of most individuals did not increase with increasing DSi availability, revealing that the Si transport system reaches the maximum speed (i.e., optimal utilization) at about 150 µM DSi and saturates at higher concentrations.

Unlike in all demosponges studied to date, the model best fitting the average DSi consumption rate of *V. pourtalesii* in response to DSi availability did not follow Michaelis-Menten kinetics (r^2 = 0.841, P = 0.004; Fig. 2A). An exponential rise to a maximum (ERM) model showed the best fit (r^2 = 0.898, P = 0.002; Fig. 2, A and B) to the empirical data on DSi consumption as a function of DSi availability, "consumption rate = a (1 – $b^{[DSi]}$)". Although the difference in statistical fit between the "Michaelis-Menten" and "ERM" models was apparently small, the ERM model was built on parameters with higher statistical significance (a = 0.093 ± 0.008, P < 0.001; b = 0.978 ± 0.006, P < 0.001) than those of the Michaelis-Menten model [V_{max} = 0.114 ± 0.019 µmol Si ml^{-1} $hour^{-1}$, P = 0.002; Michaelis constant (K_m) = 44.876 ± 23.934 µM Si, P = 0.120]. The "a" parameter of the ERM model is the exact conceptual equivalent of the V_{max} in the Michaelis-Menten model, indicating a maximum velocity of DSi utilization of 0.093 ± 0.008 µmol Si ml^{-1} $hour^{-1}$. Likewise, the exact ERM equivalent of the K_m parameter (i.e., the DSi concentration at which half-saturation or half V_{max} is achieved) can also be calculated as "[DSi] = log 0.5/log b," after having replaced in the ERM equation "consumption rate = 0.5a". It yields a value of 31.16 µM, revealing comparatively low affinity for the DSi in this sponge species (see Fig. 3).

We tested the predictions of the developed kinetic model against empirical determinations of DSi consumption and BSi production rates in field conditions. Using five custom-manufactured methyl methacrylate chambers incorporating two ROV-operated seawater collectors, we incubated four sponge individuals and a control chamber under natural settings (Fig. 1, B to D, and movies S1 and S2). Incubations were conducted in the densest sponge aggregations of both the Sambro Bank Sponge Conservation Area and LaHave Basin (fig. S1) at depths of ~160 to 185 m, respectively, for periods varying from 19 to 28 hours, and at an average DSi concentration of 15.56 ± 0.68 µM. Individuals of different sizes were assayed (64, 126, 323, and 492 ml in volume; table S3), so that a relatively wide range of the size spectrum in the natural population was considered (all but very small or very large sponges). In situ consumption rates ranged from 0.007 to 0.034 µmol Si ml^{-1} $hour^{-1}$, averaging 0.024 ± 0.012 µmol Si ml^{-1} $hour^{-1}$. This average consumption was markedly similar to the one predicted (0.027 ± 0.006 µmol Si ml^{-1} $hour^{-1}$) by the laboratory kinetics at a DSi concentration of 15.56 µM, falling within the 95% confidence range of the model (Fig. 2B).

We also estimated the rate at which BSi—that is, the siliceous skeleton—was produced by the sponges under natural conditions to compare BSi production rates to DSi consumption rates obtained both from the in situ incubations and the predictions of the laboratory kinetic model. The recovery of two moorings that were immersed for 15 and 58 months brought up sponges that had settled on them, making the approach possible (Fig. 1, G and H; Materials and Methods). The two largest sponges on the mooring deployed for 15 months were about 14 months old, 1.4 and 2.9 cm in height, 1 and 3 ml in body volume, and 0.03 and 0.11 g in BSi content, respectively. The three largest sponges on the mooring deployed for 58 months were about 54 months old and ranged from 10 to 13 cm in height, 100 to 158 ml in volume, and 3.5 to 8.3 g in BSi content. These data indicated that skeletal BSi was produced at a rate threefold higher (0.056 ± 0.008 µmol Si ml^{-1} $hour^{-1}$) during the first 14 months of life than in subsequent years (0.019 ± 0.004 µmol Si ml^{-1} $hour^{-1}$), a growth pattern also known from other aquatic invertebrates (*26*). When the data from all five individuals were pooled together, an average BSi production rate of 0.033 ± 0.021 µM Si ml^{-1} $hour^{-1}$ emerged. Again, this value fell within the 95% confidence range of the model prediction (0.029 ± 0.007 µM Si ml^{-1} $hour^{-1}$) at a DSi availability of 16.93 µM (Fig. 2B), which is the average DSi concentration in the bottom water on the central Scotian Shelf (table S4), as measured during a 20-year monitoring program (*27*). The general agreement among the rates of Si utilization predicted by the kinetic model, those measured through in situ incubations and those derived from the BSi production in field conditions, indicates consistency in the responses of the sponges in different situations, confirming that laboratory experiments are a suitable proxy for DSi utilization. It also suggests that, approximately, all consumed DSi (at least at natural ambient concentrations) becomes BSi production.

The DSi consumption kinetics of *V. pourtalesii* reaching optimal utilization at about 150 µM DSi suggests that the natural population suffers from chronic DSi limitation, as mean DSi availability in the bottom water of the central Scotian Shelf averages only 16.93 ± 8.65 µM

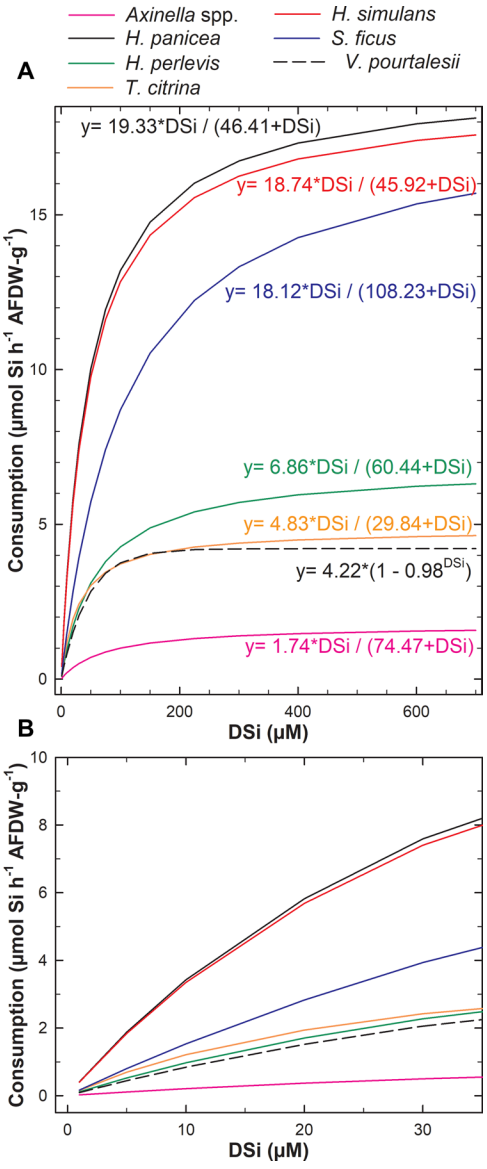

Fig. 3. Comparative summary of the DSi consumption kinetics in sponges. (**A**) The kinetics of *V. pourtalesii* is compared against all other sponge species investigated to date (*13*, *15*, *16*, *18*), which were demosponges with Michaelis-Menten kinetics. For relevant physiological comparison, DSi consumption rates were normalized to ash-free dry weight (AFDW), which represents essentially the organic component of the sponge that could be involved in silicification. The DSi consumption kinetics of *V. pourtalesii*, which does not follow a Michaelis-Menten model, is among the less efficient, except for that characterizing a group of slow-growing species in the genus *Axinella*. (**B**) A zoom on the graph within the range of natural DSi concentrations illustrates how *V. pourtalesii* is also less efficient than most demosponges at low DSi availability.

(table S4). Concentrations larger than 50 µM have not been measured at any depth in the North Atlantic (*17*). A comparison of the DSi utilization kinetics known for sponges to date (Fig. 3) indicates that *V. pourtalesii* is comparatively less efficient in DSi consumption than all demosponges but *Axinella* spp. This suggests that to build and maintain the highly silicified skeletons characterizing hexactinellid sponges, they may need continuous exposure to DSi levels higher than those characterizing the modern photic ocean [<10 µM; (*1*)]. The question remains, however, as to why the DSi consumption system of these sponges persists largely maladapted, unable to evolve in response to a shrinking DSi availability that started in the oceans at least 60 million years (Ma) ago (*19*, *28*) or even earlier (*29*).

Molecular insight into DSi consumption

To elucidate why hexactinellid sponges are particularly inefficient when using DSi at the relatively modest concentrations of the modern ocean, we attempted to activate and identify in *V. pourtalesii* (see Materials and Methods) the Si transporters potentially involved in the process of both DSi uptake and its internal transport. To this end, we quantified gene expression in six of the sponge individuals that had been exposed to progressive DSi enrichment (from 12 to 250 µM DSi) during the kinetic experiment, as indicated in the "Ex situ incubations for kinetics of DSi consumption" section. Their gene expression was contrasted with that of six individuals not exposed to any DSi enrichment but to the natural (12 to 17 µM DSi) concentration (hereafter referred to as "control individuals"). The set of treated individuals (hereafter referred to as "DSi-enriched individuals") consisted of the sponges #3, #4, #5, #7, #9, and #10 used in the kinetic experiment (as indicated in Fig. 2A).

A de novo reference transcriptome was obtained after pooling the reads from the 12 sponge libraries, and its resulting summary metrics (table S5) showed it to be well assembled and with very high BUSCO completeness scores (95.1% of the eukaryotic cassette and 87.3% of the metazoan cassette). In the DSi-enriched individuals, 597 genes were differentially up-regulated relative to the control group, of which 269 had a BLAST hit against the RefSeq and 197 against Swiss-Prot databases (fig. S2 and data file S1). In the control, 980 genes were found up-regulated when compared with the DSi-enriched individuals (fig. S2 and data file S1). Among the genes up-regulated in the DSi-enriched individuals, only 131 (33%) had a gene ontology (GO) term annotation. Identified overexpressed genes in the DSi-enriched individuals belonged to a wide array of functional categories (fig. S3 and table S5). We identified abundant transmembrane transport and vesicle-mediated transport categories, as well as responses to stress, lipid metabolism, and mRNA processing, among others in the Biological Process category. In addition, certain molecular functions were up-regulated, such as lysosome-related genes (e.g., solute carriers and cathepsins among others), transporter activity, chitin binding, and oxidoreductase activity (Fig. 4A and fig. S3). Indirect evidence indicates that silicification in sponges is a complex, energy-consuming biological process (*10*, *12*). Therefore, up-regulation of multiple gene pathways not directly related to Si utilization was not unexpected. For our study, we focused only on those genes that had previously been demonstrated in the preexisting literature of other organisms as being involved either in Si transport or in Si polymerization. This circumvents the need to carry out further unrealistic heterologous expressions or knockout experiments with *V. pourtalesii*, a deep-sea animal for which any subsequent gene functionalization would require additional unaffordable economic and logistic transnational investments for additional experimental work with live individuals.

We found two homologs of the gene *glassin*, which code for the only silicifying protein identified in hexactinellids to date (*22*). Unexpectedly, only *glassin 1* was slightly up-regulated (see Discussion) but not differentially expressed (DE), with its expression level in the DSi-enriched group being barely twofold that of the control group (Fig. 4). *Silicatein* genes, which are members of the cathepsin family

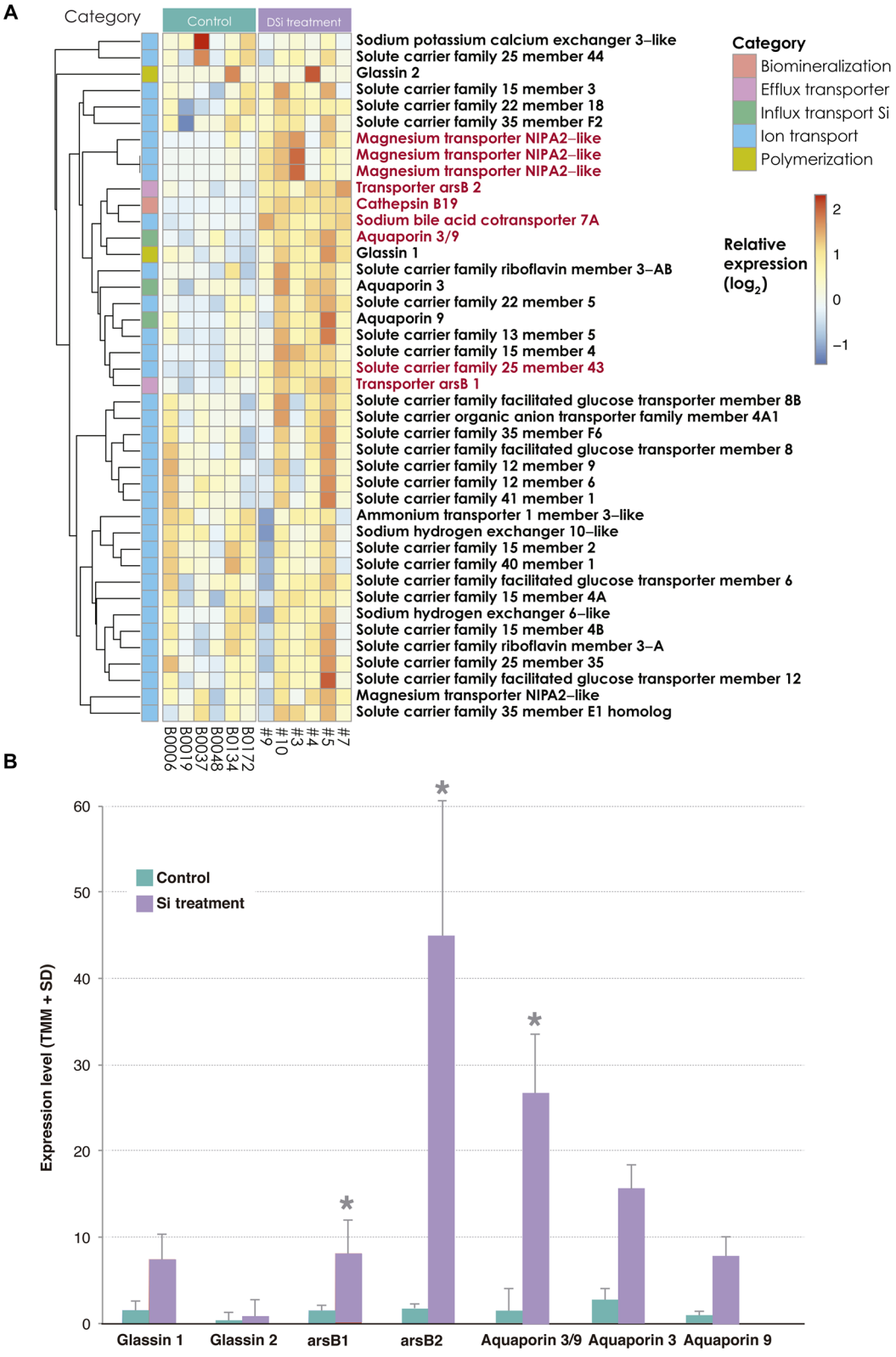

Fig. 4. Differential expression of Si-related genes in *V. pourtalesii*. (**A**) Heatmap of the genes putatively related to silicon (Si) utilization and ion transporters. Relative expression was obtained from normalized expression levels using trimmed mean of *M*-values (TMMs) of potential target genes in biomineralization. Genes DE are shown in red bold letters. (**B**) Normalized expression levels using TMMs of genes known to be involved in Si processing in sponges or other organisms. Asterisks indicate DE genes with statistical significance between the two groups of individuals (DSi-enriched group versus control group) following the criterion of at least twofold expression and a *P* value corrected by false discovery rate (FDR) of 0.001. SD, standard deviation.

of cysteine proteases and code for the silicifying enzyme of demosponges, had occasionally been reported from hexactinellids (*30*, *31*). However, no *silicatein* sequences were found in *V. pourtalesii*, a result consistent with the growing suspicion that initial reports of silicatein in hexactinellids were either contamination from demosponge samples or misidentified cathepsin-like proteins not involved in the silicification (*22*, *32*).

Two gene groups of transmembrane proteins related to Si transport (*aquaporins* and *ArsB*) were up-regulated in the DSi-enriched individuals. Aquaporins are ancient channel proteins that facilitate bidirectional passive—but relatively selective (*33*)—flux of water and/or small noncharged solutes across membranes and that are present in all kingdoms of life (*34*). The overexpressed *aquaporins* consisted of three genes (Figs. 4 and 5A). One of the *V. pourtalesii* protein sequences—aquaporin 3–like—showed high similarity to aquaglyceroporin 3 of chordates, a second one—aquaporin 9–like—was more similar to the aquaglyceroporin 9 of chordates, while a third one—aquaporin 3/9–like—had equal sequence similarity to both aquaglyceroporin 3 and 9. Only this later aquaglyceroporin 3/9 showed a much higher—and statistically significant—overexpression in the DSi-enriched individuals (Fig. 4). Aquaglyceroporins 3 and 9 are known to be major intrinsic proteins that function in chordates as passive channels facilitating a Si inflow from the intercellular medium into cells (*35*).

In a maximum likelihood (ML), noncomprehensive, phylogenetic analysis of the aquaporin protein family, which produced a tree topology with 100% congruence to that of an alternative Bayesian approach, four main clades were obtained (Fig. 5A and fig. S4): (i) one containing the aquaglyceroporins 3, 7, and 9 as well as the plant nodulin26 transporters (NOD26) and Lsi1 sequences from plants, which are all involved in passive transport of silicic acid, glycerol, and possibly water to the cells; (ii) a clade containing plasma membrane intrinsic (PIP) and tonoplast intrinsic (TIP) aquaporins, involved in water, glycerol, and ammonia transport; (iii) a clade containing aquaporin 8 (present in some sponges but not in hexactinellids) and small basic intrinsic proteins (SIP), mediating water, ammonia, and urea passive flow; and (iv) a clade of several aquaporins and PIPs involved in water transport (Fig. 5A). Only the first clade, recovering aquaglyceroporins 3, 7, and 9, showed robust nodal support.

The three *V. pourtalesii* aquaglyceroporin sequences involved in DSi transport also clustered (with statistical significance) with other unnamed aquaporins that we have recovered from the transcriptome of the hexactinellid *Rosella fibulata* and several demosponges, including both silicifying (i.e., *Lubomirskia baikalensis*, *Cliona varians*, and *Petrosia ficiformis*) and nonsilicifying species (i.e., *Dendrilla antarctica* and *Ircinia fasciculata*; see Discussion), collectively forming a robust "sponge clade" (Fig. 5A and fig. S1). While demosponges had a single member of this aquaporin clade (3, 7, and 9), hexactinellids showed expansion into three members (Fig. 5A), which could be the result of gene duplication and initial subfunctionalization for improved Si transport (see Discussion).

The other gene group related to Si utilization that was differentially overexpressed in the DSi-enriched individuals were *arsB*- and/or *Lsi2*-like genes (Figs. 4 and 5B), members of a superfamily of active ion transporters (Na^+/H^+ antiporters) that mediate a selective efflux of metalloids from the cytoplasm. The independent discovery of the *arsB* genes—initially described from bacteria as for transmembrane transporters of arsenic (*36*) and other metalloids (*37*)—and the *Lsi2* (low silicon 2) genes (*38*, *39*)—first identified in plants, as coding for transmembrane transport of Si and other metalloids—favored two different gene denominations (i.e., *arsB* versus *Lsi2*). This historical nomenclature still persists despite these genes showing clear sequence orthology and strong similarity in function (see Discussion). Two *arsB/Lsi2* genes (herein referred to as *arsB 1* and *arsB 2*) were found differentially overexpressed in *V. pourtalesii* (Fig. 4). *ArsB* genes also occur in the demosponge *Amphimedon queenslandica* and are known in several silicifying eukaryotes (Fig. 5B and fig. S4), including diatoms, radiolarians, and choanoflagellates (*23*). These eukaryotic versions of *Lsi2* and *arsB* genes also show sequence similarity to the prokaryotic arsenic transporters (Fig. 5B). In our phylogenetic hypothesis for the evolution of arsB/Lsi2 transporter proteins, in which the ML and the Bayesian approaches showed complete tree topology congruence (Fig. 5B), four main subclades were recognized among the arsB/Lsi2 proteins: (i) one consisting of the arsB homologs of bacteria, with a single arsB domain; (ii) another large clade composed by the homologs of diatoms and plants, with the diatom sequence containing a CitMHS domain [citrate-Mg^{2+}:H^+(CitM)-citrate-Ca^{2+}:H (CitH) symporter] and the plant homologs both Nhab and arsB domains; (iii) a small clade containing the Lsi2-like homologs of choanoflagellates, which only have an arsB domain; and (iv) a large clade containing the animal homologs of arsB/Lsi2, with a single CitMHS and one or several transmembrane domains.

Of note, SITs, which are sodium-coupled transmembrane proteins operating as active silicic acid–specific transporters in a variety of unicellular silicifying eukaryotes (*23*), such as diatoms, choanoflagellates, and haptophytes, were absent in *V. pourtalesii*, in agreement with other studies on sponge genomes (*23*). Related silicon transporter–like genes (*SIT-Ls*), occurring in some metazoans such as annelids, copepods, and tunicates (*23*), were also absent. Likewise, the singular active Si transporter of vertebrates, solute carrier transporter Slc34a2 (*40*), was also absent. The NBC (Na^+/HCO_3) transporter, which was tentatively suggested to be involved in cotransporting DSi in the demosponge *Suberites domuncula (24)*, was present in the transcriptome of *V. pourtalesii* (TRINITY_DN38500_c0_g1_i1) but not up-regulated by DSi enrichment, a response that does not support a direct involvement in DSi transport in this hexactinellid sponge.

DISCUSSION

Hypothesis of action mechanism for DSi transport

The results of this study suggest that molecular DSi transport in sponges appears to function through cooperation between a passive Si inflow (mediated essentially by aquaglyceroporins 3/9) and a coupled active Si efflux (mediated by the arsB transporters). Cooperation between active and passive pathways for DSi transport—but based on different transporters—has recently been found during silicification in plants (*41*) and mammals (*40*).

Aquaporins are bidirectional passive channels and, therefore, are unable to act uphill against a solute gradient. They would only be able to mediate a monodirectional Si influx effectively into the sponge cells if the DSi concentration in the seawater is high enough to build initially a steep gradient and the passive Si inflow is subsequently coupled with the active Si efflux of the arsB/Lsi2-like transporter to transport the incoming Si out of the cytoplasm. This new destination should be the mesohyl for either intercellular silicification or subsequent transport into the silicifying cells (sclerocytes) to accomplish silicification within the silica deposition vesicle of the sclerocytes (Fig. 6). Logistic constraints inherent to collecting and working

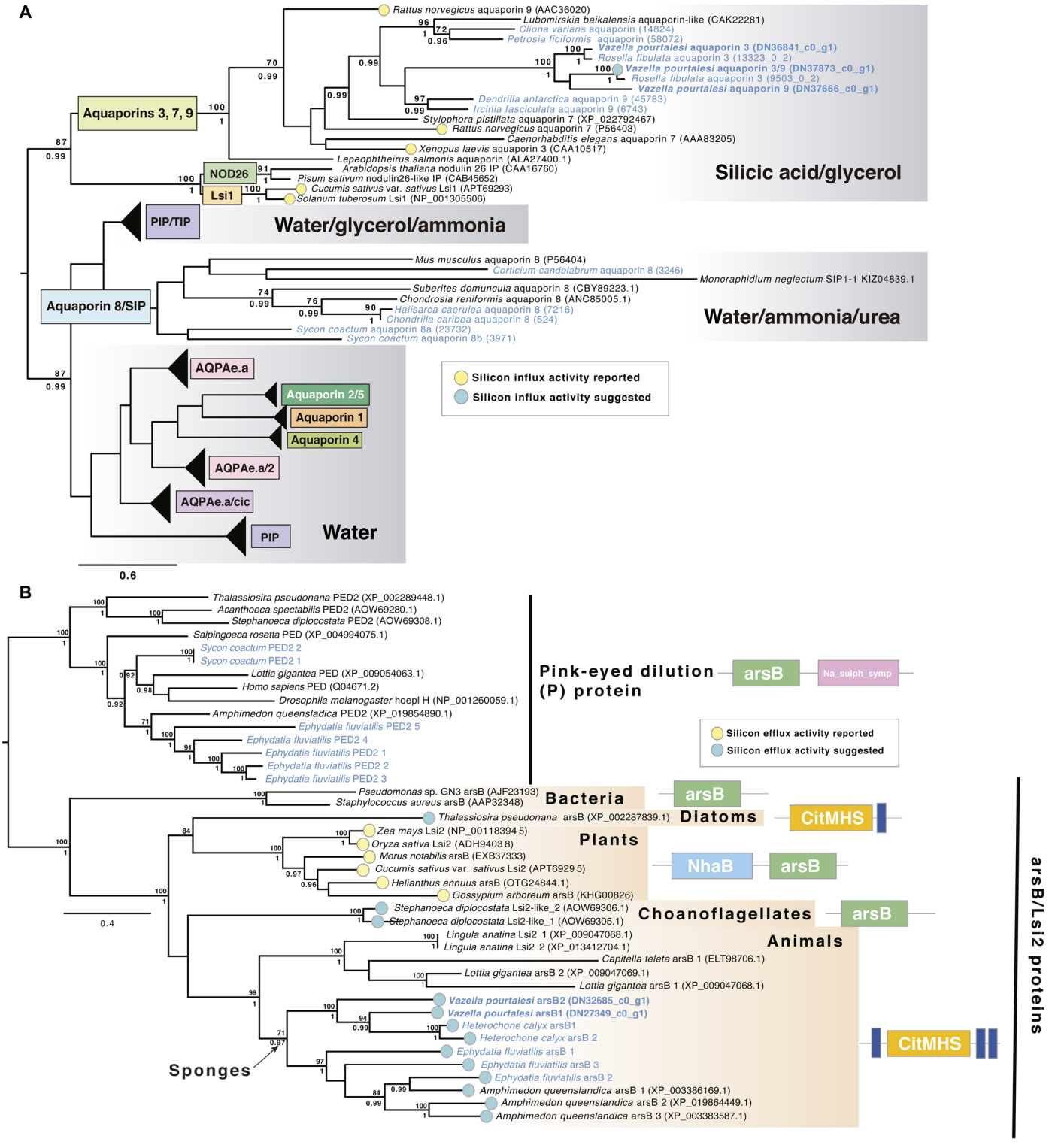

Fig. 5. Phylogenetic relationships of transmembrane silicon transporters. (**A**) Phylogenetic hypothesis of aquaporin protein family relationships and (**B**) low-silicon (Lsi2) and arsenite-antimonite (arsB) efflux transporters, which are also related to the protein family pink-eyed dilution (PED) transporters. In both cases, phylogenetic trees were obtained with ML, and the topology was congruent with that obtained from a Bayesian inference analysis. Therefore, posterior probabilities from the Bayesian inference were mapped on the nodes. Only bootstrap values more than 70 and posterior probabilities more than 0.90 are shown on the nodes. Accession numbers and contig names are in parentheses. Names in blue are new data from this study.

with living deep-sea sponges prevent further experimental work on *V. pourtalesii* in the near future to empirically resolve the exact location of the DSi membrane transporters, which is tentatively proposed in Fig. 6. Nevertheless, the information gained by this study will considerably ease future attempts to locate the DSi transporters in shallow-water demosponges, which are more accessible for experimentation. The participation of aquaporin channels explains why the consumption of DSi by sponges happens efficiently only at very high DSi concentrations: because high concentrations are needed to build initially a steep DSi concentration gradient between the extracellular and the intracellular environment. The coupling of the gradient-facilitated DSi inflow and the active Si efflux maintains the gradient steepness as the arsB transporters continuously expel DSi from the cell cytoplasm to somewhere else, either to the mesohyl or to the silica deposition vesicle (Fig. 6), depending on whether the DSi is required for intracellular or intercellular silicification. The saturation of this active arsB transporter is the most likely reason why the DSi consumption saturates at high DSi concentrations, despite those concentrations being better for passive aquaporins working more efficiently. The absence of SITs (i.e., active adenosine triphosphate–consuming transporters) in favor of passive aquaporin channels to mediate the Si influx into sponge cells and the deposition vesicle is likely the reason for the low efficiency of sponges when processing DSi at low concentrations, compared to diatoms, which do have SITs.

Physiological consequences

Our physiological results suggest that modern hexactinellids may be even less adapted than their demosponge counterparts to the relatively low DSi concentrations that characterize the modern diatom-dominated photic ocean (Fig. 3). In contrast, at DSi concentrations of <10 μM, diatoms are known to reach transport rates (*42*–*44*) that are two to three orders of magnitude those of any sponge investigated in this regard (*10*, *15*), clearly favored by their active DSi transport system based on SITs. Therefore, competitive exclusion of the hexactinellids by the better performance of diatoms and demosponges in DSi uptake is likely the main reason why hexactinellids predominate in deep-sea environments, where diatoms cannot grow because of light limitation and where DSi concentrations remain slightly higher than in the photic zone (*45*). This scenario suggests that the impressive BSi skeletons that characterize most hexactinellid sponges can only be built at slow rates (i.e., over long time periods) and when encountering DSi concentrations higher than those characterizing the upper modern ocean, which are typically less than 10 μM (*17*).

The hexactinellid *V. pourtalesii* is the only known sponge investigated to date with DSi consumption kinetics that depart from the typical Michaelis-Menten model. Further research on other hexactinellids will be needed to elucidate whether this difference consistently applies to the level of phylogenetic class. In our experimental approach to the kinetic model, we selected for the minimum number of DSi concentration steps that would identify a kinetic model with statistical significance. The reason for such tight design relates to the well-known difficulties of maintaining live deep-sea sponges under laboratory conditions for long periods. Therefore, we decided not to risk the success of the experiment unnecessarily by avoiding intermediated DSi concentrations that would have extended the duration of the assay without adding significant resolution to the essence of the outcome. Fortunately, casualties did not occur at any time during the experiment, with all sponges remaining healthy, as also reflected in the molecular message of the transcriptomes.

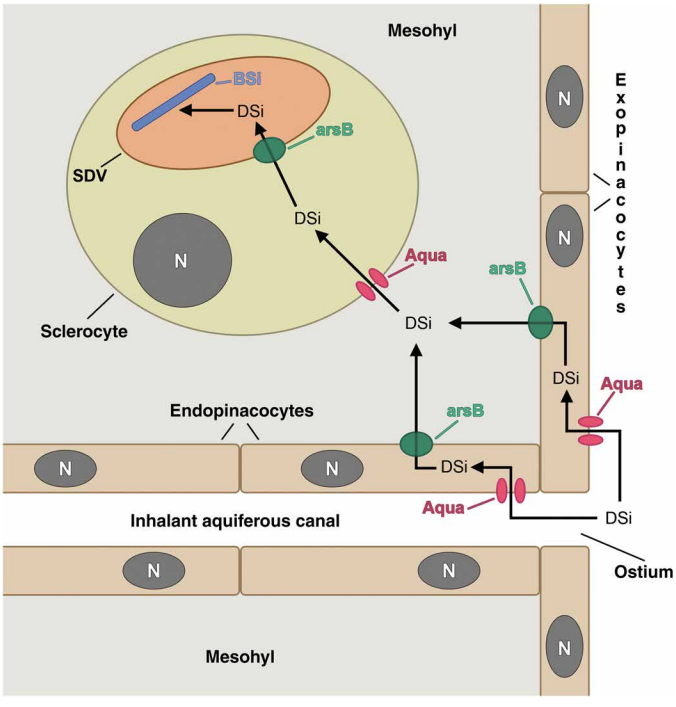

Fig. 6. Hypothesis of pathways for utilization of ambient DSi by sponges. Schematic summary of the routes putatively mediated by passive aquaglyceroporins (Aqua) and active arsB transporters across membranes of cells and the silica deposition vesicle (SDV) for BSi production. For the sake of clarity, this diagram does not include putative intercellular steps of BSi deposition and reproduces the cellular organization of demosponges rather than the syncytial structure of hexactinellids.

Molecular responses

Earlier work has demonstrated that exposure of a Mediterranean demosponge species in the laboratory to DSi concentrations much higher (30 and 100 μM) than those occurring in its natural habitat (1 μM), yields production of some types of skeletal pieces that do not occur in wild populations (*19*). In addition to revealing that skeletal production in natural conditions was chronically limited by DSi, the finding also suggested that increasing DSi up-regulates genes involved in its utilization that are not expressed at low DSi. On this basis and in the absence of further experimental progress since, we designed our experiment and focused our analysis on those genes that were overexpressed as the result of increased DSi availability. The fact that the optimal DSi utilization rate in *V. pourtalesii* was herein demonstrated to be attained at DSi concentrations between 100 and 150 μM (Fig. 2), which are not naturally available to the sponges (table S4), further encouraged the expectations of our approximation. The opposite response can be obtained in diatoms, the main Si competitors of sponges, which reach optimum DSi transport at relatively low concentrations and may down-regulate their active DSi transporters (SITs) when exposed to abnormally high DSi concentrations (*46*).

As a result of our DSi enrichment and subsequent RNA sequencing analysis, many genes related to the GO categories of vesicle- and membrane-mediated transport and lysosome transport were overexpressed, including several *lysosome-related*, *solute carriers*, *sorting nexin-1*, *transport Sec61 subunit gamma*, *BPC intracellular*

cholesterol transporter 2, *cystinosin*, *magnesium transporter NIPA2-like*, *sodium bile acid cotransporter 7 isoform 2*, *Ras-related Rab genes*, *vacuolar-sorting protein genes*, etc. However, there is no evidence to date that any of those genes are directly involved in Si utilization. Therefore, their study and functionalization fall beyond the scope of the present work. Alternatively, we obtained up-regulation of both active and passive membrane transporters that had been related to DSi transport in previous studies on organisms other than sponges.

Regarding silicifying proteins, it was interesting that the *glassin* genes (*22*), which code for the protein that catalyzes silica polycondensation in hexactinellid sponges, were not particularly overexpressed. This finding is plausible for several reasons. Experiments on freshwater demosponges showed that enzymatic axial filaments were automatically produced by the sponges even when no DSi was available in the environment to undertake spicule silicification (*47*). Likewise, high experimental DSi concentrations increased the length and thickness of spicules in a marine demosponge, but the total number of spicules (which is determined by the produced number of silicatein axial filaments) did not increase substantially (*19*). These two previous studies on demosponges agree with our results and support the view that expression of silicifying enzymes (either silicatein or glassin), unlike that of the membrane transporters (*aquaglyceroporin 3/9* and *ArsB*), may not be controlled directly by environmental DSi concentrations but is subject to more complex levels of regulation.

Regarding the passive DSi transporters, we found that *aquaglyceroporins 3* and *9* were only slightly up-regulated in DSi-enriched individuals, while *aquaglyceroporin 3/9* was significantly overexpressed (Fig. 4B). Previous evidence already has indicated that *aquaglyceroporins 3* and *9* (and also *7*) are involved in Si transport in vertebrates (*35*). The fact that homologous genes were up-regulated in the DSi-enriched individuals of *V. pourtalesii* provides strong additional evidence for their involvement in transmembrane Si transport.

Regarding the active DSi transporters, the overexpression of *arsB 1 and arsB 2* genes in the DSi-enriched individuals strongly supports their involvement in DSi transport in sponges. Such a function had already been demonstrated for other organisms, mostly land plants (*41*, *48*), but it had also tentatively been suggested—based on sequences similarity—for sponges (*23*). In rice, the same protein (but named Lsi2) has the dual capability of transporting both arsenic and Si (*41*, *48*), probably due to molecular mimicry between these two metalloids and also others, such as boron, germanium, arsenic, antimony, and tellurium (*33*). Likewise, *arsB* homologs in the diatom *Thalassiosira pseudonana* show coexpression with a silicification-related gene (*46*), suggesting that the arsB transporters, initially related to arsenic transport, can also expel actively Si across cell and vesicle membranes. ArsB/Lsi2 transporters are sister of the transporter family including pink-eyed dilution (PED) proteins (Fig. 5B), which mediate transport and processing of tyrosinase and other melanosomal proteins in melanocytes and other cells in mammals but can also transport sucrose (*49*).

Evolutionary implications for biosilicification

Collectively, evaluation of our results in the context of the available information supports the view that while Si membrane transporters appear to be shared by the two major siliceous lineages of sponges (Hexactinellida and Demospongiae), each lineage has evolved independently its own silicifying enzymes (glassin versus silicatein). This scenario also suggests that the mechanisms for Si transport across cell membranes in sponges predate the acquisition of the mechanisms for polymerizing DSi into BSi, a pattern that appears to apply to other silicifying organisms as well.

The available evidence that aquaglyceroporins 3 and 9 and arsB/Lsi2 proteins can be used for transporting, in addition to Si, other elements fundamental for survival (e.g., glycerol, several metalloids, sucrose, seawater, etc.) decreases notably the chances that those channels can be modified through evolution to improve Si transport without fatally affecting their functionality for the other elements. This is probably the reason why the DSi consumption system of siliceous sponges remained unchanged through the global DSi decrease that started at least some 100 to 65 Ma ago with the expansion of diatoms (*19*, *28*) and still persists maladapted. Yet, we have found evidence of duplication and possible subfunctionalization of aquaglyceroporins in *V. pourtalesii*. *Aquaglyceroporins 3* and *9* were only moderately up-regulated in response to the DSi treatment, while *aquaglyceroporin 3/9* was significantly overexpressed (Fig. 4). This last aquaglyceroporin could be the result of duplication and further subfunctionalization to more efficiently transport Si, while the two others remain more generalist passive transporters. It remains unknown at what level aquaglyceroporin 3/9 may still be involved in the flux of other essential metalloids.

Initially, a disconcerting feature was the presence of *aquaporin 3*–, *aquaporin 9*–, and *aquaporin 3/9*–like genes in transcriptomes of *D. antarctica* and *I. fasciculata* (Fig. 5A and fig. S4), which are nonsilicifying demosponges characterized by protein (i.e., spongin) rather than silica skeletons. The presence of those DSi passive transporters, in addition to the absence of silicatein genes in these species, has two potential explanations: (i) Passive aquaporin channels for Si, which are also used for other fundamental metalloids, were in place before the evolution of the silicifying enzymes, a hypothesis also supported by the independent acquisition of silicateins and glassin by demosponges and hexactinellids, respectively; (ii) silicatein and aquaporin channels for Si evolved concomitantly, but silicatein would have been lost secondarily and independently in various nonsilicifying members of the several demosponge lineages, while aquaporins were retained because those pore channels are also used for elements other than Si. This second option, because of invoking multiple independent loses, is less likely. Whether the silica skeleton was the primitive skeletal condition for sponges, which was subsequently lost homoplasically in several demosponge lineages, is a hypothesis that can be definitely resolved only by direct genomic evidence of the presence or absence of genes rather than only from the evidence of gene expression captured by transcriptomes. However, embryological evidence (*50*) supports the hypothesis that silica skeletons were replaced in at least some demosponge lineages through parallel evolution in favor of alternative skeletal materials (spongin, collagen, etc.). This skeletal evolution could have been forced by the drastic decrease in DSi availability triggered by the evolutionary expansion and proliferation of diatoms about 100 to 65 Ma ago, which would have operated as a negative selective pressure on siliceous skeletons (*10*, *19*). Molecular clocks could attempt to date whether the emergence of spongin skeletons (in the Verongimorpha and Keratosa subclasses) was coincidental with the expansion of diatoms or any other past event (*51*) that could have caused a drastic decrease in the availability of DSi in the upper ocean. Nevertheless, such studies have not been conducted to date.

The most unexpected aspect in the phylogenetic distribution of DSi transporters across lineages of silicifying organisms is perhaps the absence of SITs in siliceous sponges, because choanoflagellates,

which do have SITs (*23*), share a common ancestor with sponges. Likewise, SIT-L genes, which appear to be ancestral and have originated SIT genes of other silicifiers by duplication, inversion, and fusion of subunits (*52*), occur not only in several groups of silicifiers but also in some groups that are not essentially silicifiers (but rather calcifiers), such as foraminifera, coccolitophorid haptophytes, and some nonsponge metazoans. Why sponges secondarily lost the ancestral SIT complement and are now forced to transport Si through a less efficient aquaglyceroporin system remains unclear. We suggest that passive channeling is energetically less costly and could facilitate silicification even during periods of starvation or limited food supply. In a paleo-ocean with very high DSi concentrations (*53*) and moderate food supply, the replacement of active transporters by passive channeling could even be advantageous. However, when the rising activity of biosilicifiers began decreasing the environmental DSi concentration in the global paleo-ocean during the Late Mesozoic or even earlier, the lack of specialized active uptake mechanisms in favor of passive channeling became detrimental to many lineages of siliceous sponges, causing extinctions, impelling bathymetric migrations to the aphotic ocean, and forcing the skeletal evolution of siliceous sponges toward other materials to reduce their dependence on Si availability (*19*, *50*).

It is also remarkable that the *aquaglyceroporin* genes used for passive Si transport in sponges have been conserved through evolution across lineages of animals that never were—or have never been found to be—silicifiers, arriving still functional to the genome of vertebrates, where they facilitate a silicification step that has become incorporated into the general calcifying process of bone formation (*35*). This now explains why a diet rich in Si is known to favor correct bone formation in vertebrates (*54*, *55*) and why treatments based on Si also improve bone regeneration (*56*). Several lineages of demosponges contain relict species and/or genera (collectively alluded as "sclerosponges" or "coralline sponges") in which a basal skeleton of calcium carbonate coexists with isolated siliceous spicules (*57*, *58*), recalling the association between calcifying and silicifying processes recently found not only in vertebrate bone but also in cyanobacteria (*59*), coccolitophorid haptophytes (*52*), and crustaceans (*59*, *60*). Our discovery that the role in Si transport of aquaporins 3 and 9 is conserved from the Porifera to the Vertebrata gives rise to the possibility that biosilicification and biocalcification are not alternative biomineralization systems but instead mechanisms that have been functionally intertwined since the early stages of animal evolution, and perhaps even earlier.

MATERIALS AND METHODS

Species habitat, sampling, and data collection

V. pourtalesii is found at depths from 100 to 935 m along the continental margin of North America from Florida (United States) to Nova Scotia (Canada), where it forms extensive, dense aggregations in the deep basins and channels that excise the continental shelf of Nova Scotia, Canada (*8*, *25*). The aggregations are considered monospecific, consisting of an abundance of vase-shaped individuals (Fig. 1A) measuring up to 40 cm in height. Some areas of the Scotian Shelf where *V. pourtalesii* occurs more densely aggregated—i.e., forming "*Vazella* grounds"—have recently been closed (Conservation Areas; fig. S1) for protection from bottom fishing (*25*). During an oceanographic mission from 2 to 7 September 2017 to collect data from the *Vazella* grounds for the European Union–funded SponGES project, the ROV "ROPOS" was deployed from the Canadian Coast Guard Ship *Martha L Black* in the *Vazella* grounds located in the Sambro Bank Sponge Conservation Area and north of nearby LaHave Basin. ROPOS is a 40-hp Science/Work Class ROV owned and operated by the nonprofit Canadian Scientific Submersible Facility (CSSF), based in North Saanich, B.C., Canada. During deployment, forward- and downward-facing video footage of the seabed was recorded to determine the fine-scale distribution and densities of *V. pourtalesii*, and using the manipulator arms of ROPOS, live sponge individuals were collected for DSi consumption laboratory experiments and for conducting in situ incubations using benthic chambers, as described below.

Ex situ incubations for kinetics of DSi consumption

For investigating the kinetics of DSi consumption ex situ, a total of 11 sponges were collected from the Sambro Bank Sponge Conservation Area and LaHave Basin (fig. S1). The depth range of collected specimens was ~160 m in the Sambro Bank closure to 185 m north of LaHave Basin. Each sponge was collected along with the small rock on which it was attached, so that the manipulator arm of the ROV never handled the sponge tissue but just the rock (movie S1). Once on board, sponges, which were at no time exposed to air during transportation and further experimental work, were maintained for 5 days in an insulated 750-liter polyethylene holding tank inside a refrigerated container. The seawater, which was also refrigerated to 6° ± 1°C, was recirculated continuously and exchanged every 8 hours. Surface water (<5 m) was pumped using a portable pump into a tank on deck. From there, it was distributed to holding tanks inside the refrigerated container, chilled using a portable 1/3-hp chiller, and subsequently slowly pumped via a peristaltic pump (1.2 liter/min) to the tank containing the sponge specimens. The chilled water tank was refilled twice a day, resulting in four water exchanges/day in the sponge holding tank. The sponges, which were attached to a small rock in all cases, were maintained on the bottom of the holding tank by placing them within individual compartments of a polyviniyl chloride (PVC) grid. Upon return to the Bedford Institute of Oceanography (BIO) in Dartmouth, Nova Scotia, the sponges were transferred to a 500-liter aquarium for 24 hours. The saltwater intake at BIO is 200 m from shore and at a depth of 17 m (~3 m off bottom). The seawater was passed through a sand filter and then a 20-μm (nominal) bag filter before being delivered to the lab. The filtered seawater entered a 1000-liter aerated tank (header tank) where it was heated/chilled to ~6° to 9°C. This water was then gravity-fed into the sponge holding tank (500 liters of insulated polyethylene). Flow rates were maintained at ~3 to 5 liter/min. A small magnetic drive pump was added to the bottom of the holding tank to provide circulation and horizontal flow across the sponges. The pump was modified with a 12.5 mm–by–300 mm vertical pipe with 6-mm holes added to provide horizontal flow.

Upon initiation of the ex situ experimentation, sponges attached to their respective rocky substratum were transferred to a 360-liter tank (hereafter referred to as the "preconditioning tank") and left there for 24 hours for acclimation to a refrigerated (9° ± 0.5°C) seawater system with recirculation. To characterize the kinetic pattern, DSi consumption by the sponges under increasing DSi availability was measured. The experiment ended when saturation was reached by the sponges, that is, when an increase in DSi availability did not stimulate any further increase in the rate of DSi consumption. Seven levels of DSi concentration were progressively offered to the 11 assayed sponges: 12 (approximate field values), 30, 60, 100, 150, 200, and

250 μM Si. Under each concentration, sponges were incubated separately in a polypropylene 16-liter container (hereafter referred to as the "incubation aquaria") for 24 hours. Before each 24-hour incubation, sponges were maintained in the preconditioning tank for 24 hours. Thus, the approach consisted of an alternation of 24-hour "preconditioning" and "incubation" periods for 2 weeks (from 9 to 22 September 2017). The alternation of preconditioning and incubating steps had three main purposes. The first was to facilitate the survival of the sponges across the battery of incubations in the relatively small (16 liters) incubating aquaria, an objective successfully met, as there were no casualties over the course of the 2-week experiment. Second, to render the approach conservative, during each preconditioning step, the sponges were exposed for 24 hours to the same DSi concentration that was to be assayed in the following incubation. Therefore, during the preconditioning step, the sponges were able to take up as much DSi as needed to satisfy their chronic avidity for DSi, an approach that has been empirically demonstrated to lead to slightly lower DSi consumption rates during the following 24-hour incubation period (*15*). Third, the sum of the duration of the preconditioning period and the incubation period collectively provided a total time of exposure to each DSi concentration long enough (48 hours) to allow the sponges to unfold a complete physiological response in the silicification process. Theoretically, such a response is expected to involve the generation of new populations of silicifying cells to deal with the increasing availability of DSi, the activation of new sets of genes, and the completion of massive production of silicifying proteins (*10*, *19*). Along with the 11 assayed sponges, we used three control aquaria, each containing seawater and a rock as the one used by the sponges for attachment, but with no sponge. These controls served to correct for potential processes of either DSi release from the rocks or DSi precipitation at the rock surface. It was also difficult to obtain exactly the intended DSi concentrations in the large preconditioning tank because the transfer of sponges to it upon conclusion of each incubation involved an unavoidable transference of seawater at a lower DSi concentration, causing minor dilution of the concentration in the preconditioning tank. This logistical constraint resulted in the following concentrations during the incubations: 12.5, 30.4, 59.0, 93.0, 141.6, 191.8, and 234.0 μM Si.

The seawater used for the experiments was pumped in from the Bedford Basin, Nova Scotia (at 7°C) and filtered on a 1-μm mesh, a pore size small enough to prevent the passage of planktonic DSi users (e.g., diatoms, radiolarians, etc.) but allowing, in part, the passage of natural sponge food, that is, the smallest bacterioplankton. In addition, we fed the sponges during the entire experiment by adding 35 ml of a DSi-free, concentrated culture (approximately 10^6 cells/ml) of the haptophyte *Isochrysis galbana* to the 360-liter tank at the beginning of each preconditioning step. We assumed that, after passing repetitively throughout the mechanical water pump, part of the microphytoplankton cells would be lysed, resulting in a mix of particulate and dissolved organic matter available to the sponges.

The assayed DSi concentrations were prepared by adding the corresponding volume of a buffered 0.1 M sodium metasilicate solution [Na_2SiO_3 (pH 10)] to the 360 liters of filtered seawater contained in the preconditioning tank, followed by mixing of the water for 18 hours with a submersible pump to ensure complete molecular diffusion before transferring the sponges to the tank for their corresponding preconditioning period. To determine the rate of DSi utilization by the assayed sponges during the incubations at each DSi concentration step, a 50-ml water sample was collected at the beginning and end of each 24-hour incubation period. Seawater samples, collected using acid-cleaned plastic syringes, were immediately filtered through 0.22-μm pore, polycarbonate syringe filters (Millex-GS Millipore) and stored in the fridge no longer than 2 days until analysis. Samples from the same DSi concentration step were analyzed together into a single analysis using a Technicon AutoAnalyzer 3 (AA3, SEAL Analytical), a service provided by the CERC.OCEAN research group based at the Dalhousie University (Halifax, Nova Scotia, Canada). Analyses were run in triplicate following the standard colorimetric method, with a determination accuracy (as percent error) of <5%. Samples with a DSi concentration higher than 60 μM were diluted before analysis with artificial seawater prepared with the same salinity as the water samples (35 practical salinity unit). The rate of DSi utilization by a sponge at a given DSi availability was inferred by calculating the difference in DSi concentration between the start and end of an incubation and after correcting by the average concentration change (often negligible) that occurred in the set of control aquaria.

At the end of the experiment, we measured the volume (ml) of both the assayed individuals and their rock substratum by water displacement. Sponges were subsequently wet-weighed (g), dried at 60°C to a constant dry weight (g), and combusted at 540°C for 10 hours for ash-free dry weight (AFDW; g). Rates of DSi consumption were normalized by sponge volume (ml) and/or AFDW (g), volume of seawater in the incubating aquaria (liters) after discounting sponge and rock volume, and duration of the incubation (hours). We preferentially expressed data normalized to sponge volume because it facilitates their future applicability to field sponge populations using ROV images without the need of collecting individuals. However, for correct physiological between-species comparison, we used normalization by AFDW. The relationship between normalized DSi consumption rates (in μmol Si ml^{-1} $hour^{-1}$or g^{-1}) and DSi availability (μM) was analyzed by nonlinear regression to identify the best-fitting model for the empirical observations.

In situ incubations for DSi consumption

We built five benthic incubation chambers using methylmethacrilate and inox steel, with an incubation volume of either 17.3 or 13.3 liters (Fig. 1, B to D). Chambers incorporated a floor piece of Delrin acetal resin (Fig. 1B), which allowed for the incubation of sponges in isolation from the external environment, thus avoiding interference by nutrient fluxes from sediments that may be resuspended during deployment. The chambers incorporated two external sampling bottles (120 ml) made of steel and internally folded with polytetrafluoroethylene. Through a steel capillary (20 cm long and 0.6 mm wide) that pierced the wall of the chamber, each bottle was designed to collect a water sample (under negative pressure conditions) from inside the incubation chamber while it was opened for 5 min and then closed using the ROV manipulator arms (movies S1 and S2).

During the 2017 oceanographic mission on the Canadian Coast Guard Ship *Martha L Black*, four sponges and a control treatment were incubated in situ. Sponges were collected along with the small rock to which they were attached using the manipulator arms of the ROV (movie S1). Each sponge was then placed on the floor piece and covered with the chamber so that the chamber rested into a groove on the floor piece designed to seal the unit from leakages. Once the sponge was inside the chamber and the chamber was properly sealed, one of the sampling bottles was opened to collect water for 5 min and then closed again to avoid water exchange with the surrounding

medium (movie S2). As a control, we incubated a rock selected from the sponge grounds but without an attached sponge. After an incubation period of 19 to 28 hours (incubation time varied because of weather and the logistics of the cruise), the ROV returned to the chambers and triggered the second sampling bottle. After this second water collection, the sponge and its attachment substrate were collected to estimate volume and biomass and to normalize DSi consumption rate, as indicated in the above section of "Ex situ incubations for kinetics of DSi consumption." Seawater samples were processed for determination of the initial and final DSi concentrations and deriving consumption rate as described in the above section.

Individual BSi production in the natural habitat

We aimed to estimate how much BSi—mass of siliceous skeleton—was produced by the sponges in their natural habitat per unit time to serve as a comparison for the predictions of DSi consumption from the laboratory-based kinetic model. Preliminary field work revealed that *V. pourtalesii* biofouled acoustic mooring arrays deployed by the Ocean Tracking Network (OTN; Dalhousie University) from Halifax to the shelf break on the Scotian Shelf (Fig. 1, E and F). During routine servicing of these arrays, *V. pourtalesii* individuals were recovered from two moorings that had been immersed for 15 and 58 months, and rates of sponge growth and BSi production during those two periods were estimated. During an additional recovery made during a 2018 oceanographic mission, several substrata offered for *V. pourtalesii* settlement about ~1 year before brought out no sponge recruits (SponGES Consortium, unpublished information). It suggested that larval release is likely to occur in July to August. Therefore, the two largest sponges on the mooring immersed for 15 months were estimated to be 14 months old, and the three largest sponges on the 58-month-old mooring were estimated to be 54 months old. After determining their volume, sponges were wet-weighed (g), dried at 60°C to a constant dry weight (g), and combusted at 540°C for 10 hours for AFDW (g). The BSi content was estimated as 95% of the ash weight. However, for comparative purposes, the BSi content of some of the larger sponges was also estimated through the loss of weight before and after desilicification of the sample in 5% hydrofluoric acid.

Gene expression and phylogenetic analyses

We collected tissue samples from six control individuals collected from Emerald Basin and from six DSi-enriched individuals (#3, #4, #5, #7, #9, and #10) used in the kinetic experiment (tables S2 and S3). Approximately 5 cm^3 of tissue sample was collected immediately upon termination of the kinetic experiment, when concentrations were 250 μM DSi, and before any further processing of the sponges for morphometric studies. Samples were preserved in RNAlater (Ambion) at 4°C for 24 hours and then stored at −80°C until further processing. Total RNA from each sample was extracted using a TRIzol (Thermo Fisher Scientific, UK) standard extraction followed by a polyA selection of mRNA using a Dynabeads Direct mRNA purification kit (Thermo Fisher Scientific, UK) according to the manufacturer's protocols. These were used to produce an RNA library for next-generation sequencing using the ScriptSeq library prep kit v2 provided by Illumina (CA, USA). Sequencing was performed on a single run of the Illumina NextSeq 500 platform by the Natural History Museum's (London, UK) Sequencing Unit at 2 × 150 bp read length. A total of 202,315,355 reads were sequenced and remained after the removal of adaptor sequence and initial quality screening. We visualized the quality across the sequencing reads using FastQC (Babraham Bioinformatics) and performed additional trimming with Trimmomatic (*61*) to remove areas of sequence with low Phred scores and any residual sequences shorter than 36 bp (settings: ILLUMINACLIP:/ScriptSeq_adapters.fa:2:30:10 LEADING:3 TRAILING:3 HEADCROP:8 SLIDINGWINDOW:4:15 MINLEN:36, where ScriptSeq_adapters.fa contained the sequences of the adaptors used in sequencing). The remaining total of 173,280,196 paired reads (unpaired reads were not retained) were then used to construct a transcriptome using Trinity 2.4.0 (*62*) with default options. Raw reads can be accessioned at the Short Read Archive (SRA) under BioProject number PRJNA580361.

Annotation and gene expression analyses

We obtained the annotations for our de novo–assembled transcriptome using "BlastX" command in DIAMOND (*63*) against two different databases: RefSeq and Swiss-Prot (last accessed in August to September 2018), retaining only the best hit with an *e*-value threshold of 10^{-5} in both cases. Then, we used Blast2GO (*64*) to obtain the GO terms associated with the blast hits obtained against Swiss-Prot for Biological Process, Molecular Function, and Cellular Component, with the GOSlim function. Completeness of the transcriptome was assessed by searching for single-copy orthologs in both eukaryotic and metazoan databases using BUSCO (*65*).

For the gene expression analysis, we used standard mapping strategies Bowtie2 and RSEM (RNA-Seq by Expectation Maximization) as implemented in Trinity to collect the number of reads aligning with each of our genes in the reference transcriptome and then used the raw count reads against each gene to perform the differential gene expression analysis using edgeR (*66*) as implemented in Trinity. We only retained the genes with a corrected *P* value of false discovery rate (FDR) of 0.001 and at least fourfold expression (-P 1e-3 -C 2). The DE genes were annotated using the gene IDs from Swiss-Prot and also the GO terms (see table S2). To visualize the GO categories enriched in our DE genes, we used REVIGO (*67*) and plotted circos plots in the R statistical software program.

The expression levels of target genes involved in silica production for spicule building in hexactinellids (polymerization and biomineralization: *glassin* and *cathepsins*; ion transporters: *transporters arsB*, *aquaporins 3* and *9*, *solute carriers*, *magnesium transporters NIPA*, *ammonia transporters*, *sodium-potassium calcium exchanger*, and *sodium bile acid cotransporter*) were collected from the normalized expression values using trimmed mean of *M*-value (TMM) matrix obtained with edgeR and plotted using pheatmap in R.

Phylogenetic analyses

In our phylogenetic analysis of aquaporins and arsB transporters in *V. pourtalesii*, we included sequences of all major groups of aquaporins and arsenite-antimonite efflux protein sequences collected from GenBank and our transcriptomic databases for sponges (see accession numbers in Fig. 5, fig. S4, and data file S1). Phylogenetic analyses of the genes coding for the passive and active transporters were conducted separately, with ingroup and outgroup sequences selected on previous knowledge of the protein families—aquaporins (*34*) and arsB/Lsi2 transporters (*49*). All sequences were aligned with MAFFT v5 (*68*), and the phylogenetic trees were built with RAxML 8.1.22 (*69*) with Le-Gascuel as the protein model of substitution and GAMMAI correction for rate variation among sites as obtained from PROTTEST

(*70*) using the Akaike information criterion. Reliability of the phylogenetic trees was estimated using 100 bootstrap replicates. As a congruence test for the previous ML-based phylogenies, a subsequent Bayesian phylogenetic analysis was conducted for both protein families, using MrBayes (*71*) v3.2.2 x64 with the model provided by PROTTEST. The Monte Carlo Markov Chain search was run over at least 20,000,000 generations. Trees were sampled every 2500 generations, and the first 25% of trees gathered were discarded as "burn-in." Convergence was checked with Tracer 1.7 (*72*).

SUPPLEMENTARY MATERIALS

Supplementary material for this article is available at http://advances.sciencemag.org/cgi/content/full/6/28/eaba9322/DC1

View/request a protocol for this paper from *Bio-protocol*.

REFERENCES AND NOTES

1. P. Tréguer, D. M. Nelson, A. J. Van Bennekom, D. J. DeMaster, A. Leynaert, B. Quéguiner, The silica balance in the world ocean: A reestimate. *Science* **268**, 375–379 (1995).
2. P. Tréguer, P. Pondaven, Global change. Silica control of carbon dioxide. *Nature* **406**, 358–359 (2000).
3. P. J. Tréguer, C. L. De La Rocha, The world ocean silica cycle. *Ann. Rev. Mar. Sci.* **5**, 477–501 (2013).
4. T. L. Simpson, B. E. Volcani, *Silicon and Siliceous Structures in Biological Systems* (Springer-Verlag, 1981).
5. K. Thamatrakoln, M. Hildebrand, Silicon uptake in diatoms revisited: A model for saturable and nonsaturable uptake kinetics and the role of silicon transporters. *Plant Physiol.* **146**, 1397–1407 (2008).
6. A. Leynaert, S. N. Longphuirt, P. Claquin, L. Chauvaud, O. Ragueneau, No limit? The multiphasic uptake of silicic acid by benthic diatoms. *Limnol. Oceanogr.* **54**, 571–576 (2009).
7. C. A. Durkin, J. A. Koester, S. J. Bender, E. V. Armbrust, The evolution of silicon transporters in diatoms. *J. Phycol.* **52**, 716–731 (2016).
8. M. Maldonado, R. Aguilar, R. J. Bannister, J. J. Bell, K. W. Conway, P. K. Dayton, C. Díaz, J. Gutt, M. Kelly, E. L. R. Kenchington, S. P. Leys, S. A. Pomponi, H. T. Rapp, K. Rützler, O. S. Tendal, J. Vacelet, C. M. Young, Marine animal forests, *in The Ecology of Benthic Biodiversity Hotspots*, S. Rossi, L. Bramanti, A. Gori, C. Orejas, Eds. (Springer International Publishing, 2017), pp. 145–183.
9. J. W. F. Chu, M. Maldonado, G. Yahel, S. P. Leys, Glass sponge reefs as a silicon sink. *Mar. Ecol. Prog. Ser.* **441**, 1–14 (2011).
10. M. Maldonado, M. Ribes, F. C. van Duyl, Nutrient fluxes through sponges: Biology, budgets, and ecological implications. *Adv. Mar. Biol.* **62**, 113–182 (2012).
11. M. Maldonado, M. López-Acosta, C. Sitjà, M. García-Puig, C. Galobart, G. Ercilla, A. Leynaert, Sponge skeletons as an important sink of silicon in the global oceans. *Nat. Geosci.* **12**, 815–822 (2019).
12. H. Frøhlich, D. Barthel, Silica uptake on the marine sponge *Halichondria panicea* in Kiel Bight. *Mar. Biol.* **128**, 115–125 (1997).
13. M. Maldonado, L. Navarro, A. Grasa, A. Gonzalez, I. Vaquerizo, Silicon uptake by sponges: A twist to understanding nutrient cycling on continental margins. *Sci. Rep.* **1**, 30 (2011).
14. M. López-Acosta, A. Leynaert, V. Coquille, M. Maldonado, Silicon utilization by sponges: An assessment of seasonal changes. *Mar. Ecol. Prog. Ser.* **605**, 111–123 (2018).
15. M. López-Acosta, A. Leynaert, J. Grall, M. Maldonado, Silicon consumption kinetics by marine sponges: An assessment of their role at the ecosystem level. *Limnol. Oceanogr.* **63**, 2508–2522 (2018).
16. M. López-Acosta, A. Leynaert, M. Maldonado, Silicon consumption in two shallow-water sponges with contrasting biological features. *Limnol. Oceanogr.* **61**, 2139–2150 (2016).
17. J. Sarmiento, N. Gruber, *Ocean Biogeochemical Dynamics* (Princeton Univ. Press, 2006).
18. T. Reincke, D. Barthel, Silica uptake kinetics of *Halichondria panicea* in Kiel Bight. *Mar. Biol.* **129**, 591–593 (1997).
19. M. Maldonado, M. C. Carmona, M. J. Uriz, A. Cruzado, Decline in mesozoic reef-building sponges explained by silicon limitation. *Nature* **401**, 785–788 (1999).
20. M. Maldonado, A. Riesgo, A. Bucci, K. RÜ tzlerb, Revisiting silicon budgets at a tropical continental shelf: Silica standing stocks in sponges surpass those in diatoms. *Limnol. Oceanogr.* **55**, 2001–2010 (2010).
21. K. Shimizu, J. Cha, G. D. Stucky, D. E. Morse, Silicatein α: Cathepsin L-like protein in sponge biosilica. *Proc. Natl. Acad. Sci. U.S.A.* **95**, 6234–6238 (1998).
22. K. Shimizu, T. Amano, M. R. Bari, J. C. Weaver, J. Arima, N. Mori, Glassin, a histidine-rich protein from the siliceous skeletal system of the marine sponge *Euplectella*, directs silica polycondensation. *Proc. Natl. Acad. Sci. U.S.A.* **112**, 11449–11454 (2015).
23. A. O. Marron, S. Ratcliffe, G. L. Wheeler, R. E. Goldstein, N. King, F. Not, C. de Vargas, D. J. Richter, The evolution of silicon transport in eukaryotes. *Mol. Biol. Evol.* **33**, 3226–3248 (2016).
24. H.-C. Schröder, S. Perović-Ottstadt, M. Rothenberger, M. Wiens, H. Schwertner, R. Batel, M. Korzhev, I. M. Müller, W. E. G. Müller, Silica transport in the demosponge *Suberites domuncula*: Fluorescence emission analysis using the PDMPO probe and cloning of a potential transporter. *Biochem. J.* **381**, 665–673 (2004).
25. L. Beazley, Z. Wang, E. Kenchington, I. Yashayaev, H. T. Rapp, J. R. Xavier, F. J. Murillo, D. Fenton, S. Fuller, Predicted distribution of the glass sponge *Vazella pourtalesi* on the scotian shelf and its persistence in the face of climatic variability. *PLOS One* **13**, e0205505 (2018).
26. A. G. Hirst, J. Forster, When growth models are not universal: Evidence from marine invertebrates. *Proc. Biol. Sci.* **280**, 20131546 (2013).
27. B. Petrie, P. Yeats, P. Strain, Nitrate, silicate and phosphate atlas for the Scotian shelf and the gulf of Maine, in *Canadian Technical Report of Hydrography and Ocean Sciences* (Fisheries and Oceans Canada, Dartmouth, Canada, 1999).
28. R. G. Maliva, A. H. Knoll, R. Siever, Secular change in chert distribution: A reflection of evolving biological participation in the silica cycle. *Palaios* **4**, 519–532 (1989).
29. G. Fontorbe, P. J. Frings, C. L. De La Rocha, K. R. Hendry, D. J. Conley, A silicon depleted North Atlantic since the Palaeogene: Evidence from sponge and radiolarian silicon isotopes. *Earth Planet. Sci. Lett.* **453**, 67–77 (2016).
30. W. E. G. Müller, X. Wang, K. Kropf, A. Boreiko, U. Schlossmacher, D. Brandt, H. C. Schröder, M. Wiens, Silicatein expression in the hexactinellid *Crateromorpha meyeri*: The lead marker gene restricted to siliceous sponges. *Cell Tissue Res.* **333**, 339–351 (2008).
31. W. E. G. Müller, A. Boreiko, U. Schloßmacher, X. Wang, C. Eckert, K. Kropf, J. Li, H. C. Schröder, Identification of a silicatein(-related) protease in the giant spicules of the deep-sea hexactinellid *Monorhaphis chuni*. *J. Exp. Biol.* **211**, 300–309 (2008).
32. G. N. Veremeichik, Y. N. Shkryl, V. P. Bulgakov, S. V. Shedko, V. B. Kozhemyako, S. N. Kovalchuk, V. B. Krasokhin, Y. N. Zhuravlev, Y. N. Kulchin, Occurrence of a silicatein gene in glass sponges (Hexactinellida: Porifera). *Mar. Biotechnol.* **13**, 810–819 (2011).
33. G. P. Bienert, M. D. Schüssler, T. P. Jahn, Metalloids: Essential, beneficial or toxic? Major intrinsic proteins sort it out. *Trends Biochem. Sci.* **33**, 20–26 (2008).
34. R. Zardoya, Phylogeny and evolution of the major intrinsic protein family. *Biol. Cell* **97**, 397–414 (2005).
35. A. P. Garneau, G. A. Carpentier, A.-A. Marcoux, R. Frenette-Cotton, C. F. Simard, W. Rémus-Borel, L. Caron, M. Jacob-Wagner, M. Noël, J. J. Powell, R. Bélanger, F. Côté, P. Isenring, Aquaporins mediate silicon transport in humans. *PLOS One* **10**, e0136149 (2015).
36. B. P. Rosen, Families of arsenic transporters. *Trends Microbiol.* **7**, 207–212 (1999).
37. B. P. Rosen, The role of efflux in bacterial resistance to soft metals and metalloids. *Essays Biochem.* **34**, 1–15 (1999).
38. J. F. Ma, K. Tamai, N. Yamaji, N. Mitani, S. Konishi, M. Katsuhara, M. Ishiguro, Y. Murata, M. Yano, A silicon transporter in rice. *Nature* **440**, 688–691 (2006).
39. J. Acosta, E. Ancochea, M. Canals, M. J. Huertas, E. Uchupi, Early pleistocene volcanism in the emile baudot seamount, balearic promontory (western mediterranean sea). *Mar. Geol.* **207**, 247–257 (2004).
40. S. Ratcliffe, R. Jugdaohsingh, J. Vivancos, A. Marron, R. Deshmukh, J. F. Ma, N. Mitani-Ueno, J. Robertson, J. Wills, M. V. Boekschoten, M. Müller, R. C. Mawhinney, S. D. Kinrade, P. Isenring, R. R. Bélanger, J. J. Powell, Identification of a mammalian silicon transporter. *Am. J. Physiol. Cell Physiol.* **312**, C550–C561 (2017).
41. J. F. Ma, N. Yamaji, A cooperative system of silicon transport in plants. *Trends Plant Sci.* **20**, 435–442 (2015).
42. E. Paasche, Silicon and the ecology of marine plankton diatoms. II. Silicate-uptake kinetics in five diatom species. *Mar. Biol.* **19**, 262–269 (1973).
43. H. L. Conway, P. J. Harrison, Marine diatoms grown in chemostats under silicate or ammonium limitation. IV Transient response of *Chaetoceros debilis*, *Skeletonema costatum* and *Thalassiosira gravida* to a single addition of the limiting nutrient. *Mar. Biol.* **43**, 33–43 (1977).
44. V. Martin-Jézéquel, M. Hildebrand, M. A. Brzezinski, Silicon metabolism in diatoms: Implications for growth. *J. Phycol.* **36**, 821–840 (2000).
45. D. M. Nelson, P. Tréguer, M. A. Brzezinski, A. Leynaert, B. Quéguiner, Production and dissolution of biogenic silica in the ocean: Revised global estimates, comparison with regional data and relationship to biogenic sedimentation. *Global Biogeochem. Cycles* **9**, 359–372 (1995).
46. R. P. Shrestha, M. Hildebrand, Evidence for a regulatory role of diatom silicon transporters in cellular silicon responses. *Eukaryot. Cell* **14**, 29–40 (2014).
47. C. Yourassowsky, R. Rasmont, The differentiation of sclerocytes in fresh-water sponges grown in a silica-poor medium. *Differentiation* **25**, 5–9 (1984).
48. J. F. Ma, N. Yamaji, N. Mitani, X.-Y. Xu, Y.-H. Su, S. P. McGrath, F.-J. Zhao, Transporters of arsenite in rice and their role in arsenic accumulation in rice grain. *Proc. Natl. Acad. Sci. U.S.A.* **105**, 9931–9935 (2008).
49. H. Meyer, O. Vitavska, H. Wieczorek, Identification of an animal sucrose transporter. *J. Cell Sci.* **124**, 1984–1991 (2011).

50. M. Maldonado, Embryonic development of verongid demosponges supports the independent acquisition of spongin skeletons as an alternative to the siliceous skeleton of sponges. *Biol. J. Linn. Soc.* **97**, 427–447 (2009).
51. K. R. Hendry, A. O. Marron, F. Vincent, D. J. Conley, M. Gehlen, F. M. Ibarbalz, B. Quéguiner, C. Bowler, Competition between silicifiers and non-silicifiers in the past and present ocean and its evolutionary impacts. *Front. Mar. Sci.* **5**, 22 (2018).
52. G. M. Durak, A. R. Taylor, C. E. Walker, I. Probert, C. de Vargas, S. Audic, D. Schroeder, C. Brownlee, G. L. Wheeler, A role for diatom-like silicon transporters in calcifying coccolithophores. *Nat. Commun.* **7**, 10543 (2016).
53. R. G. Maliva, A. H. Knoll, B. M. Simonson, Secular change in the precambrian silica cycle: Insights from chert petrology. *Geol. Soc. Am. Bull.* **117**, 835–845 (2005).
54. E. M. Carlisle, Silicon in bone formation, in *Silicon and siliceous structures in biological systems*, T. L. Simpson, B. E. Volcani, Eds. (Springer Verlag, 1981), pp. 69–94.
55. S. Wang, X. Wang, F. G. Draenert, O. Albert, H. C. Schröder, V. Mailänder, G. Mitov, W. E. G. Müller, Bioactive and biodegradable silica biomaterial for bone regeneration. *Bone* **67**, 292–304 (2014).
56. M. Arora, E. Arora, The promise of silicon: Bone regeneration and increased bone density. *J. Arthros. Joint Surg.* **4**, 103–105 (2017).
57. P. Willenz, W. D. Hartman, Micromorphology and ultrastructure of caribbean sclerosponges. *Mar. Biol.* **103**, 387–401 (1989).
58. J. Vacelet, S. C. Morris, J. D. George, R. Gibson, H. M. Platt, *The Origins and Relationships of Lower Invertebrates* (Clarendon Press, 1985), vol. 28, pp. 1–13.
59. N. B. Matsko, N. Žnidaršič, I. Letofsky-Papst, M. Dittrich, W. Grogger, J. Štrus, F. Hofer, Silicon: The key element in early stages of biocalcification. *J. Struct. Biol.* **174**, 180–186 (2011).
60. J. Michels, J. Vogt, S. N. Gorb, Tools for crushing diatoms—Opal teeth in copepods feature a rubber-like bearing composed of resilin. *Sci. Rep.* **2**, 465 (2012).
61. A. M. Bolger, M. Lohse, B. Usadel, Trimmomatic: A flexible trimmer for illumina sequence data. *Bioinformatics* **30**, 2114–2120 (2014).
62. M. G. Grabherr, B. J. Haas, M. Yassour, J. Z. Levin, D. A. Thompson, I. Amit, X. Adiconis, L. Fan, R. Raychowdhury, Q. Zeng, Z. Chen, E. Mauceli, N. Hacohen, A. Gnirke, N. Rhind, F. di Palma, B. W. Birren, C. Nusbaum, K. Lindblad-Toh, N. Friedman, A. Regev, Full-length transcriptome assembly from RNA-Seq data without a reference genome. *Nat. Biotechnol.* **29**, 644–652 (2011).
63. B. Buchfink, C. Xie, D. H. Huson, Fast and sensitive protein alignment using DIAMOND. *Nat. Methods* **12**, 59–60 (2014).
64. A. Conesa, S. Götz, J. M. García-Gómez, J. Terol, M. Talón, M. Robles, Blast2GO: A universal tool for annotation, visualization and analysis in functional genomics research. *Bioinformatics* **21**, 3674–3676 (2005).
65. F. A. Simão, R. M. Waterhouse, P. Ioannidis, E. V. Kriventseva, E. M. Zdobnov, BUSCO: Assessing genome assembly and annotation completeness with single-copy orthologs. *Bioinformatics* **31**, 3210–3212 (2015).
66. M. D. Robinson, D. J. McCarthy, G. K. Smyth, edgeR: A bioconductor package for differential expression analysis of digital gene expression data. *Bioinformatics* **26**, 139–140 (2009).
67. F. Supek, M. Bošnjak, N. Škunca, T. Šmuc, REVIGO summarizes and visualizes long lists of gene ontology terms. *PLOS One* **6**, e21800 (2011).
68. K. Katoh, G. Asimenos, H. Toh, Bioinformatics for DNA Sequence Analysis, *Methods in Molecular Biology (Methods and Protocols)*, D. Posada, Ed. (Humana Press, 2019), vol. 537, pp. 29–64.
69. A. Stamatakis, RAxML version 8: A tool for phylogenetic analysis and post-analysis of large phylogenies. *Bioinformatics* **30**, 1312–1313 (2014).
70. F. Abascal, R. Zardoya, D. Posada, ProtTest: Selection of best-fit models of protein evolution. *Bioinformatics* **21**, 2104–2105 (2005).
71. F. Ronquist, J. P. Huelsenbeck, MrBayes 3: Bayesian phylogenetic inference under mixed models. *Bioinformatics* **19**, 1572–1574 (2003).
72. A. Rambaut, A. J. Drummond, D. Xie, G. Baele, M. A. Suchard, Posterior summarization in Bayesian phylogenetics using tracer 1.7. *Syst. Biol.* **67**, 901–904 (2018).

Acknowledgments: We thank B. MacDonald for help with logistics during sponge collection and maintenance in experimental conditions, C. Sitjà for help with sponge dry and ash weights, and M. García-Puig for video editing; F. Whoriskey and J. Pratt of the (OTN, Dalhousie University) for the collection of specimens from the OTN moorings; G. Yahel (Ruppin Academic Center) for advice when building the seawater collectors of the incubation chambers. **Funding:** This research was completed mostly by funds from the SponGES H2020 grant (BG-01-2015.2, agreement number 679849-2) to M.M. and A.R. and from Fisheries and Oceans Canada Strategic Program for Ecosystem-Based Research and Advice (SPERA) and International Governance Strategy (IGS) projects awarded to L.B. and E.K. This study also benefitted from funding by a PBS grant (MINECO CTM2015-67221-R) to M.M. This study is in memory of Hans Tore Rapp, who passed away on 7 March 2020, and who was the main coordinator of the H2020 SponGES project that has made this research possible. **Author contributions:** M.M. designed the study. The physiological experiments and nutrient analyses were performed and analyzed by M.M. and M.L.-A. E.K. and L.B. dealt with mapping, collection of organisms, and the logistics of cruise organization and laboratory gearing for in vivo experimentation with deep-sea sponges and nutrient analysis. A.R. and V.K. conducted the transcriptomic analysis, the analysis of differential gene expression, and the phylogenetic analyses, being the molecular data interpreted by M.M. and A.R. M.M. assembled the first draft of manuscript, which was further refined through invaluable contributions by all authors. **Competing interests:** The authors declare that they have no competing interests. **Data and materials availability:** All data and access numbers needed to evaluate the conclusions in the paper are present in the paper and/or the Supplementary Materials. Raw transcript reads can be accessioned at the SRA under BioProject number PRJNA580361. Additional data related to this paper may be requested from the authors.

Submitted 16 January 2020
Accepted 22 May 2020
Published 8 July 2020
10.1126/sciadv.aba9322

Citation: M. Maldonado, M. López-Acosta, L. Beazley, E. Kenchington, V. Koutsouveli, A. Riesgo, Cooperation between passive and active silicon transporters clarifies the ecophysiology and evolution of biosilicification in sponges. *Sci. Adv.* **6**, eaba9322 (2020).